

Quantum teleportation with a complete Bell state measurement

YOON-HO KIM*, SERGEI P. KULIK†, and YANHUA SHIH
Department of Physics, University of Maryland, Baltimore County,
Baltimore, Maryland 21250, USA

(Received 29 March, 2001; revision received 19 July 2001)

Abstract. By using the quantum teleportation protocol, Alice can send an *unknown* quantum state (e.g. the polarization of a single photon) to Bob without ever knowing about it. This paper discusses a quantum teleportation experiment in which nonlinear interactions are used for the Bell state measurement. Since the Bell state measurement is based on nonlinear interactions, *all* four Bell states can be distinguished. Therefore, teleportation of a polarization state can occur with certainty, in principle. Details of the theory and the experimental set-up are discussed.

1. Introduction

Suppose that two distant parties, Alice and Bob, want to share some information. For example, Alice possesses a physical system which contains the information (it may be a page of a quantum mechanics textbook) and she wants to give this information to Bob who is far apart from Alice. Let us also assume that Alice cannot send the physical system itself to Bob, but she can communicate with Bob through a classical communication channel.

If this information is classical, the process is easy. Alice first has to learn the information by making a ‘measurement’; she reads the page of the textbook she wants to send to Bob. By knowing the information, she can then communicate with Bob through a classical communication channel to recite the information. This process is possible since we can make an accurate measurement on a classical system.

However, if the system is quantum mechanical, for example, a single photon or an electron, the above process cannot work; there is in general no way of measuring the state of a single quantum system without destroying the original state. For example, if there is only *one* photon with *unknown* polarization, a single measurement on the photon cannot give us any useful information of the polarization state of the photon. If one can make copies of the quantum system, then the state of the system can be determined *statistically* by making repeated measurements on the clones of the quantum system. Unfortunately, perfect ‘cloning’ cannot be done on a quantum system. This is due to so-called ‘no cloning theorem’ [1]. The no

*Present address: Oak Ridge National Laboratory, P.O. Box 2008, Oak Ridge, TN 37831-6355, USA; e-mail: kimy@ornl.gov; tel: +1-865-241-0921; fax: +1-865-241-0381

†Permanent address: Dept of Physics, Moscow State University, Moscow, Russia.

cloning theorem states that one cannot make an exact copy of an arbitrary quantum state. This is an essential feature of quantum information: it cannot be duplicated at will, unlike classical information.

Let us review the no cloning theorem briefly, as discussed by Wootters and Zurek [1]. Suppose that there is a perfect cloning machine and the polarization state of the initial photon is $|\downarrow\rangle$ or $|\leftrightarrow\rangle$. Then

$$|A_0\rangle|\downarrow\rangle \rightarrow |A_v\rangle|\downarrow, \downarrow\rangle,$$

$$|A_0\rangle|\leftrightarrow\rangle \rightarrow |A_h\rangle|\leftrightarrow, \leftrightarrow\rangle,$$

where $|A_0\rangle$ is the initial state of the cloning machine, $|A_h\rangle$ and $|A_v\rangle$ are the final states, and $|\downarrow\rangle$ and $|\leftrightarrow\rangle$ refer to the vertical and horizontal polarization state of a single photon, respectively. $|\downarrow, \downarrow\rangle$ represents the state in which two photons (the original photon and the cloned photon) are both polarized vertically.

If the incoming photon has an arbitrary polarization given by $\alpha|\downarrow\rangle + \beta|\leftrightarrow\rangle$, the ideal cloning machine performs the following operation.

$$|A_0\rangle(\alpha|\downarrow\rangle + \beta|\leftrightarrow\rangle) \rightarrow \alpha|A_v\rangle|\downarrow, \downarrow\rangle + \beta|A_h\rangle|\leftrightarrow, \leftrightarrow\rangle.$$

If the final states of the cloning machine $|A_v\rangle$ and $|A_h\rangle$ are not identical, the two outgoing photons are in a mixed state. If the final states are identical, then the two emerging photons are in the pure state

$$\alpha|\downarrow, \downarrow\rangle + \beta|\leftrightarrow, \leftrightarrow\rangle. \quad (1)$$

In neither of the two cases do the two outgoing photons have the same polarization state as the incoming photon $\alpha|\downarrow\rangle + \beta|\leftrightarrow\rangle$. In the case of successful cloning, i.e. the cloned photon has the same polarization as the incoming photon, the state should have the form

$$\frac{1}{\sqrt{2}}(\alpha a_v^\dagger + \beta a_h^\dagger)^2|0\rangle = \alpha^2|\downarrow, \downarrow\rangle + \frac{1}{\sqrt{2}}\alpha\beta|\downarrow, \leftrightarrow\rangle + \beta^2|\leftrightarrow, \leftrightarrow\rangle, \quad (2)$$

where a_v^\dagger and a_h^\dagger are the creation operators of the photon in vertical polarization and horizontal polarization, respectively. Clearly, equation (2) is different from equation (1).

From the above arguments, it can be seen that one can indeed clone or amplify two orthogonal polarizations, if they are known beforehand. This means that the linearity of quantum mechanics does not prohibit the amplification of any orthogonal set of quantum states if a cloning device is specifically designed for those states. However, no cloning machine which will amplify an arbitrary polarization (or quantum state) exists. Similarly, if one knows the polarization of a single photon beforehand, one can measure it. However, if one is given a single photon without knowledge of its polarization, there is no way of telling the polarization state of a single photon by making a measurement.

Suppose now that Alice has a single photon with unknown polarization. The polarization of a single photon can be used to encode quantum information. Since Alice does not and cannot know the exact polarization of her photon, there is no classical way of giving this polarization information to Bob. Keep in mind that Alice cannot send the photon directly to Bob. Recently, Bennett and co-workers devised a scheme of 'quantum teleportation' which allows Alice to send an *unknown* state of her quantum particle to Bob, if Alice and Bob share entangled

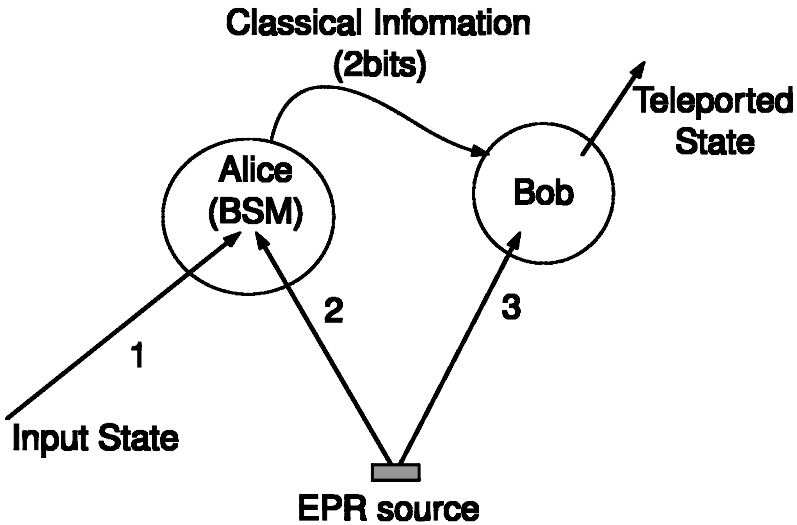


Figure 1. Cartoon showing how quantum teleportation works. Alice and Bob share entangled particle pairs (EPR pair). Alice makes Bell state measurement (BSM) on her EPR particle (particle 2) and the input particle (particle 1). She then communicates with Bob through a classical channel. Bob then makes an appropriate unitary transformation on his EPR particle (particle 3) depending on Alice's measurement result. The quantum state of particle 1 is then 'teleported' to particle 3.

particle pairs [2, 3]. Neither Alice nor Bob has to know the quantum state itself. The unknown quantum state of Alice's particle is 'teleported' to Bob's particle once quantum teleportation process is completed. However, the information transfer is not instantaneous since quantum teleportation requires both quantum and classical channels.[†]

The basic features of quantum teleportation are shown in figure 1. Alice and Bob share entangled particle pairs (or EPR pairs), particle 2 and particle 3 [3]. Alice wants to teleport the unknown state of her particle 1 to Bob. She first makes a special measurement called Bell state measurement (BSM) on her particle 1 and particle 2. She then tells the result of the Bell state measurement to Bob through a classical channel. Knowing the result of Alice's Bell state measurement, Bob can make a certain unitary transformation on his particle 3 to obtain the exact replica of the quantum state of particle 1. Again, the special feature of quantum teleportation is that neither Alice nor Bob knows the state of the particle and the teleportation is not instantaneous.

2. Quantum teleportation with a complete Bell state measurement

As mentioned in Section 1, the idea of quantum teleportation is to utilize the nonlocal correlations between an Einstein–Podolsky–Rosen pair of particles to

[†] The nonlocal quantum correlation between the entangled particle pair shared by Alice and Bob establishes the quantum channel. The classical channel can be established by using any presently known communication method, such as telephone. Since the speed of information transfer through any classical channel is limited by the speed of light c , quantum teleportation cannot be used for superluminal communication.

prepare a quantum system in some state, which is the exact replica of an arbitrary unknown state of a distant individual system [2, 3]. Recently, three groups of physicists in Europe and the USA reported experiments in this direction [4–6]. This paper reviews the details of a quantum teleportation experiment which has been reported in [7].

Ideally, a quantum teleportation experiment should satisfy the following conditions:

- (i) the input quantum state must be an *arbitrary* state;
- (ii) there must be an output quantum state which is a ‘copy’ of the input state;
- (iii) the Bell state measurement (BSM) must be able to distinguish the complete set of the orthogonal Bell states so that the input state can be teleported with certainty;
- (iv) for any input quantum state the teleportation must be deterministic and not statistical.

The experiment described here satisfies all of the above conditions [7]. The input state is an *arbitrary polarization state* and the BSM can distinguish *all* four orthogonal Bell states so that the state has a 100% certainty to be teleported in principle. This is because the BSM is based on nonlinear interactions which are *necessary* and *nontrivial* physical processes for correlating the input state and the entangled EPR pair [8–12].

Note that we consider measurements of polarization entanglement only. If one assumes measurements of entanglement in more than one degree of freedom, nonlinear interactions may not be necessary for a complete BSM, see [13]. However, as pointed out by Lütkenhaus *et al.*, ‘half the job is already done’ in the latter case [12].

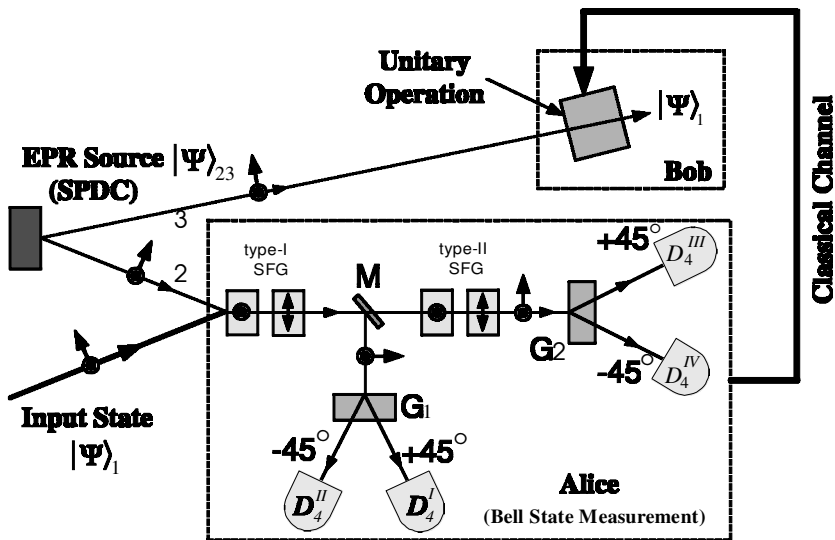


Figure 2. Principle schematic of quantum teleportation with a complete BSM. Nonlinear interactions (SFG) are used to perform the BSM. \odot and \uparrow represent the respective horizontal and vertical orientations of the optic axes of the crystals.

The four essential parts, just as the original protocol [2], of the experiment are shown in figure 2:

- (1) the input quantum state which is an arbitrary polarization state (qubit),
- (2) the EPR pair,
- (3) Alice (who performs the BSM of the input state and her EPR particle), and
- (4) Bob (who carries out unitary operations on his EPR particle).

Let us now discuss the details of how the experiment works. The input quantum state is an *arbitrary polarization state* given by,

$$|\Psi_1\rangle = \alpha|0_1\rangle + \beta|1_1\rangle, \quad (3)$$

where $|\alpha|^2 + |\beta|^2 = 1$. $|0\rangle$ and $|1\rangle$ represent the two orthogonal linear polarization bases $|H\rangle$ (horizontal) and $|V\rangle$ (vertical), respectively. The EPR pair shared by Alice and Bob is prepared by spontaneous parametric down-conversion (SPDC) as,

$$|\Psi_{23}\rangle = \frac{1}{\sqrt{2}}\{|0_20_3\rangle - |1_21_3\rangle\}, \quad (4)$$

with the subscripts 2 and 3 as labelled in figure 2. Note that any one of the four Bell states can be used for this purpose. The complete state of the three particles before Alice's measurement is then,

$$|\Psi_{123}\rangle = \frac{\alpha}{\sqrt{2}}\{|0_10_20_3\rangle - |0_11_21_3\rangle\} + \frac{\beta}{\sqrt{2}}\{|1_10_20_3\rangle - |1_11_21_3\rangle\}. \quad (5)$$

The four Bell states which form a complete orthonormal basis for both particle 1 and particle 2 are usually represented as,

$$|\Phi_{12}^{\pm}\rangle = \frac{1}{\sqrt{2}}\{|0_10_2\rangle \pm |1_11_2\rangle\},$$

$$|\Psi_{12}^{\pm}\rangle = \frac{1}{\sqrt{2}}\{|0_11_2\rangle \pm |1_10_2\rangle\}.$$

State (5) can now be rewritten in the following form based on the above orthonormal Bell states,

$$\begin{aligned} |\Psi_{123}\rangle = & \frac{1}{2}\{|\Phi_{12}^{(+)}\rangle(\alpha|0_3\rangle - \beta|1_3\rangle) + |\Phi_{12}^{(-)}\rangle(\alpha|0_3\rangle + \beta|1_3\rangle) \\ & + |\Psi_{12}^{(+)}\rangle(-\alpha|1_3\rangle + \beta|0_3\rangle) + |\Psi_{12}^{(-)}\rangle(-\alpha|1_3\rangle - \beta|0_3\rangle)\}. \end{aligned} \quad (6)$$

To teleport the state of particle 1 to particle 3 reliably, Alice must be able to distinguish her four Bell states by means of the BSM performed on particle 1 and her EPR particle (particle 2). She then tells Bob through a classical channel to perform a corresponding linear unitary operation on his EPR particle (particle 3) to obtain an exact replica of the state of particle 1. This completes the process of quantum teleportation.

Unfortunately, distinguishing between the four polarization Bell states is not trivial. Recently, Lütkenhaus, Calsamiglia, and Suominen [12] and Vaidman and Yoran [11] independently showed that nonlinear interactions are required to distinguish all four polarization Bell states. Since then several methods have been proposed to teleport the polarization state of a photon reliably [14–17].

Complete Bell state measurement is also useful for quantum dense coding [18, 19], entanglement swapping [20, 21], etc.

The proposed Bell state measurement scheme shown in figure 2 is based on nonlinear interactions: optical sum frequency generation (SFG) (or ‘up-conversion’). Four SFG nonlinear crystals are used for ‘measuring’ and ‘distinguishing’ the complete set of the four Bell states. Photon 1 and photon 2 may interact either in the two type-I crystals or in the two type-II crystals to generate a higher frequency photon (labelled as photon 4). The projection measurements on photon 4 (either at the 45° or at the 135° direction) correspond to the four Bell states of photon 1 and photon 2, $|\Phi_{12}^{(\pm)}\rangle$ and $|\Psi_{12}^{(\pm)}\rangle$.

Let us now discuss the BSM in detail (see figure 2). The first type-I SFG crystal converts two $|V\rangle$ polarized photons $|1_1 1_2\rangle$ into a single horizontal polarized photon $|H_4\rangle$. Similarly, the second type-I SFG crystal converts two $|H\rangle$ polarized photons $|0_1 0_2\rangle$ into a single vertical polarized photon $|V_4\rangle$. The first and the last terms on the right-hand side in equation (5) thus become,

$$|\Psi_{43}\rangle = \alpha|V_4 0_3\rangle - \beta|H_4 1_3\rangle.$$

Dichroic beamsplitter M reflects only SFG photons to the 45° polarization projector G_1 . Two detectors D_4^I and D_4^{II} are placed at the 45° and 135° output ports of G_1 , respectively. Denoting the 45° and 135° polarization bases by $|45^\circ\rangle$ and $|135^\circ\rangle$, the state $|\Psi_{43}\rangle$ may be rewritten as,

$$|\Psi_{43}\rangle = \frac{1}{\sqrt{2}}\{|45^\circ\rangle_4^I(\alpha|0_3\rangle - \beta|1_3\rangle) + |135^\circ\rangle_4^I(\alpha|0_3\rangle + \beta|1_3\rangle)\}, \quad (7)$$

i.e. if detector D_4^I (45°) is triggered, the quantum state of Bob’s EPR photon (photon 3) is:

$$|\Psi_3\rangle = \alpha|0_3\rangle - \beta|1_3\rangle, \quad (8)$$

and, if detector D_4^{II} (135°) is triggered, the quantum state of Bob’s photon is:

$$|\Psi_3\rangle = \alpha|0_3\rangle + \beta|1_3\rangle. \quad (9)$$

As we have analysed above, the 45° and the 135° polarized type-I SFG components in equation (7) correspond to the superposition of $|0_1 0_2\rangle$ and $|1_1 1_2\rangle$, which are the respective Bell states $|\Phi_{12}^{(+)}\rangle$ and $|\Phi_{12}^{(-)}\rangle$, i.e.

$$\begin{aligned} |45^\circ\rangle_4^I &= \frac{1}{\sqrt{2}}(|V\rangle_4 + |H\rangle_4) \\ &= \frac{1}{\sqrt{2}}(|0_1 0_2\rangle + |1_1 1_2\rangle) \\ &= |\Phi_{12}^{(+)}\rangle, \end{aligned} \quad (10)$$

and

$$\begin{aligned}
|135^\circ\rangle_4^I &= \frac{1}{\sqrt{2}}(|V\rangle_4 - |H\rangle_4) \\
&= \frac{1}{\sqrt{2}}(|0_1 0_2\rangle - |1_1 1_2\rangle) \\
&= |\Phi_{12}^{(-)}\rangle.
\end{aligned} \tag{11}$$

Similarly, the other two Bell states are distinguished by the type-II SFGs. The states $|0_1 1_2\rangle$ and $|1_1 0_2\rangle$ are made to interact in the first and the second type-II SFG crystals respectively to generate a higher frequency photon with either horizontal (the first type-II SFG) or vertical (the second type-II SFG) polarization. A 45° polarization projector G_2 is used after the type-II SFG crystals and two detectors D_4^{III} and D_4^{IV} are placed at the 45° and the 135° output ports of G_2 , respectively. On the new bases of 45° and 135° for the SFG photon, the second and the third terms on the right-hand side in equation (5) thus become,

$$|\Psi_{43}\rangle = \frac{1}{\sqrt{2}}\{ |45^\circ\rangle_4^{II}(-\alpha|1_3\rangle + \beta|0_3\rangle) + |135^\circ\rangle_4^{II}(-\alpha|1_3\rangle - \beta|0_3\rangle)\}, \tag{12}$$

i.e. if detector D_4^{III} (45°) is triggered, the quantum state of Bob's photon is:

$$|\Psi_3\rangle = -\alpha|1_3\rangle + \beta|0_3\rangle, \tag{13}$$

and if detector D_4^{IV} (135°) is triggered, the quantum state of Bob's photon is:

$$|\Psi_3\rangle = -\alpha|1_3\rangle - \beta|0_3\rangle. \tag{14}$$

The 45° and the 135° polarized type-II SFG components correspond to the superposition of $|0_1 1_2\rangle$ and $|1_1 0_2\rangle$ which are the Bell states $|\Psi_{12}^{(+)}\rangle$ and $|\Psi_{12}^{(-)}\rangle$ respectively, i.e.

$$\begin{aligned}
|45^\circ\rangle_4^{II} &= \frac{1}{\sqrt{2}}(|V\rangle_4 + |H\rangle_4) \\
&= \frac{1}{\sqrt{2}}(|0_1 1_2\rangle + |1_1 0_2\rangle) \\
&= |\Psi_{12}^{(+)}\rangle,
\end{aligned} \tag{15}$$

and

$$\begin{aligned}
|135^\circ\rangle_4^{II} &= \frac{1}{\sqrt{2}}(|V\rangle_4 - |H\rangle_4) \\
&= \frac{1}{\sqrt{2}}(|0_1 1_2\rangle - |1_1 0_2\rangle) \\
&= |\Psi_{12}^{(-)}\rangle.
\end{aligned} \tag{16}$$

To obtain the exact replica of the state of equation (3), Bob needs simply to perform a corresponding unitary transformation after learning from Alice which of her four detectors, D_4^I , D_4^{II} , D_4^{III} , or D_4^{IV} , has triggered.

To demonstrate the working principle of this scheme, we measure the joint detection rates between detectors $D_4^I-D_3$, $D_4^{II}-D_3$, $D_4^{III}-D_3$, and $D_4^{IV}-D_3$, where D_3 is Bob's detector (see figure 5). In these measurements we choose the input state $|\Psi_1\rangle$

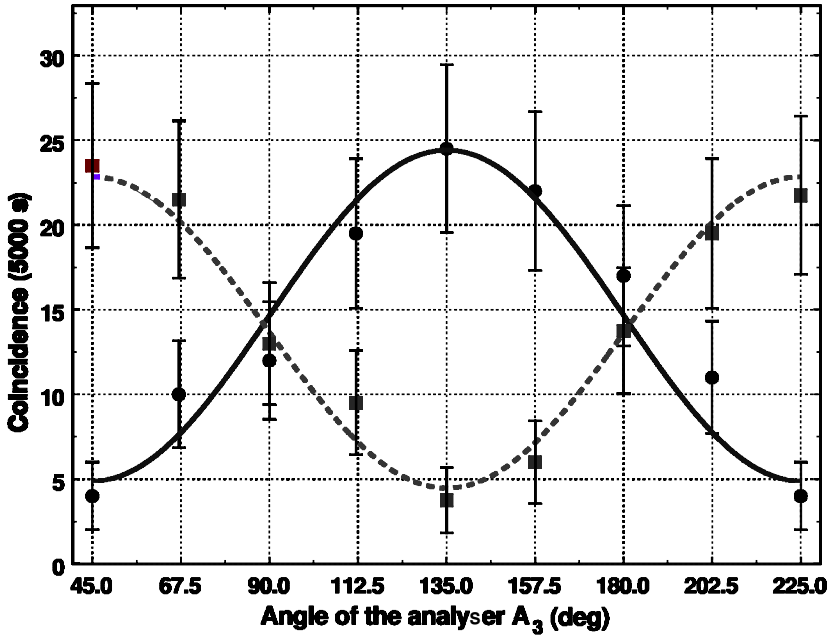


Figure 3. Teleportation data using type-I SFG. Solid line (●) is the joint detection rate $D_4^I - D_3$ for 45° linear polarization as an input state. Dashed line (■) is for $D_4^{II} - D_3$ for the same input state. The expected π phase shift is clearly demonstrated.

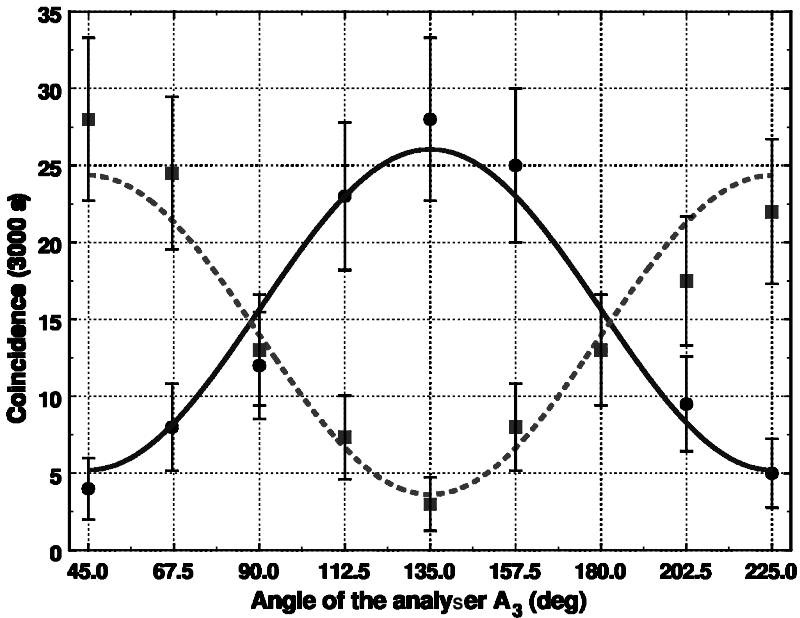


Figure 4. Teleportation data using type-II SFG. Solid line (●) is the joint detection rate $D_4^{III} - D_3$ and dashed line (■) is for $D_4^{IV} - D_3$. Again, the expected π phase shift is clearly demonstrated.

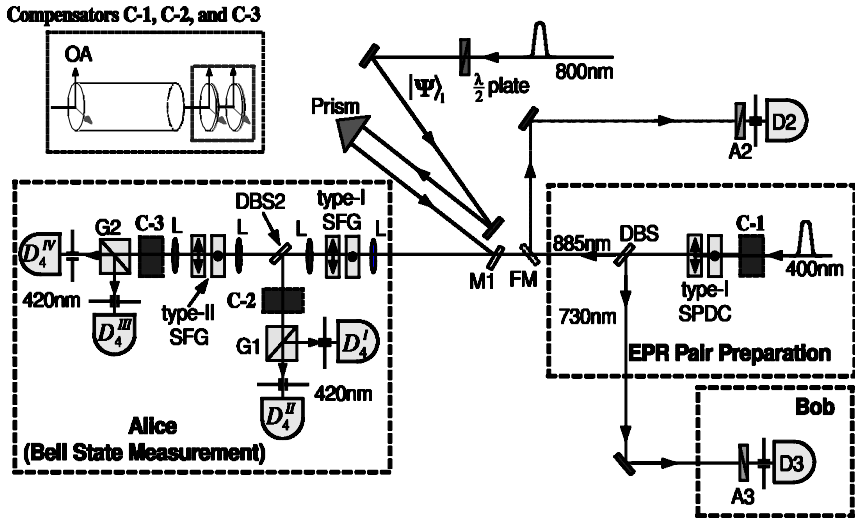


Figure 5. Experimental setup. The inset shows the details of the compensators. A_2 and A_3 are the polarization analyzers. See text for details.

as a linear polarization state. For a fixed input polarization state, the angle of the polarization analyser A_3 which is placed in front of Bob's detector is rotated and the joint detection rates are recorded. Figure 3 shows two typical data sets for $D_4^I - D_3$ and $D_4^{II} - D_3$. The input polarization state is 45° . Clearly, these data curves confirm equations (8) and (9). The different phases of the two curves reflect the phase difference between equations (8) and (9). Experimental data for $D_4^{III} - D_3$ and $D_4^{IV} - D_3$ show similar behaviour, see figure 4, which confirms equations (13) and (14).

3. Experimental set-up: input state and EPR source

The schematic of the experimental set-up is shown in figure 5. The input polarization state is prepared by using a $\lambda/2$ plate from a femtosecond laser pulse (pulse width ≈ 100 fs and central wavelength = 800 nm). In the present experiment, the input state is a polarization state of a femtosecond laser pulse which contains approximately 10^{10} photons in each pulse. However, only one of them actually has a chance to take part in the SFG process since Alice's share of the EPR pair is in the single photon state. It can also be shown that every photon in the input laser pulse has the polarization state of equation (3) by considering the correspondence principle. What is being 'teleported' is the polarization state or qubit associated with this photon which actually took part in the SFG process.

One may argue that the state of the laser beam is *collectively* in a coherent state which is a product state in the coherent state representation. However, the concept of the state of the system is different from that of the polarization of the field. The polarization state of the single photon that actually takes part in the SFG process is given by equation (3). This result can also be obtained through the weak-field approximation of a coherent state for the photon in the Fock state basis.

In this experiment, a femtosecond laser pulse was used instead of a single photon as an input due to the low efficiency of SFG at the single photon level. This means that many photons of the same polarization state have been prepared and used as the input. In principle, one can use a single photon qubit as an input state in our scheme. Due to the low efficiency of SFG, however, one needs to wait a much longer time for teleportation to occur. This means that one would still need to prepare many photons in the identical state for one teleportation experiment since the experiment has to be repeated many times. Therefore, for the proof-of-principle demonstration of quantum teleportation with a complete Bell state measurement, it does not matter which option an experimentalist takes if the efficiency of the Bell state measurement (or SFG process) is very low. Note, however, that if quantum teleportation is to be useful in quantum communication and quantum computing in the future, it is imperative that such a measurement be made with nearly perfect efficiency with a single photon state as an input. We are currently studying ways to improve the efficiency of nonlinear optics at the single-photon level.

The EPR pair (730 nm–885 nm photon pair) is generated by two nondegenerate type-I SPDCs. The optical axes of the first and the second SPDC crystals are oriented in the respective horizontal (\odot) and vertical (\downarrow) directions. The SPDC crystals are pumped by a 45° polarized 100 fs laser pulse with 400 nm central wavelength. The BBO crystals (each with thickness 3.4 mm) are cut for collinear nondegenerate phase matching. Since the two crystals are pumped equally, the SPDC pair can be generated either in the first BBO as $|V_{885}\rangle_2|V_{730}\rangle_3$ ($|1_21_3\rangle$) or in the second BBO as $|H_{885}\rangle_2|H_{730}\rangle_3$ ($|0_20_3\rangle$) with equal probability (885 and 730 refer to the wavelengths in nanometres). In order to prepare an EPR state in the form of equation (4) (a Bell state), these two alternatives have to be quantum mechanically ‘indistinguishable’ and have the expected relative phase. A Compensator (C-1) is used for this purpose and it consists of two parts: a thick quartz rod and two thin plates. The thick quartz rod is used to compensate the time delay between the two amplitudes $|1_21_3\rangle$ and the $|0_20_3\rangle$, and two thin quartz plates are used to adjust the relative phase between them by an angular tilting. See [23, 24] for the details of the compensator C-1.

A dichroic beamsplitter *DBS* is placed behind the SPDC crystals to separate and send the photon 2 (885 nm) and photon 3 (730 nm) to Alice and Bob, respectively. To check the EPR state, a flipper mirror *FM* is used to send the photon 2 (885 nm) to a photon-counting detector D_2 for EPR correlation measurement. Both the space-time and polarization correlations must be checked before teleportation measurements, in order to be certain of having high degree EPR entanglement and the expected relative phase between the $|1_21_3\rangle$ and the $|0_20_3\rangle$ amplitudes (see [22–24] for details).

Figure 6 shows the space-time and polarization interference observed between the detectors D_2 and D_3 (Bob). The observed high-visibility quantum interference means that the photon pairs that are shared by Alice and Bob have high degrees of entanglement. The EPR state $|\Phi^{(-)}\rangle$ is prepared by setting the space-time phase so that the coincidence counts between the two detectors are at the minimum (destructive interference). Once the EPR state in equation (4) is prepared, *FM* is flipped-down and photon 2 (885 nm) is given to Alice for BSM with photon 1.

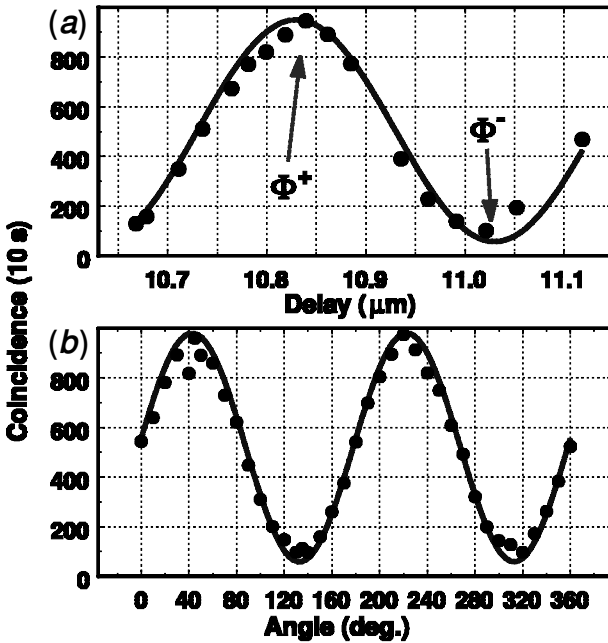


Figure 6. Space-time and polarization interference between the detectors D_2 and D_3 (Bob). (a) Space-time interference by varying the pump phase when $\theta_2 = \theta_3 = 45^\circ$. Transition from $|\Phi^{(+)}\rangle$ to $|\Phi^{(-)}\rangle$ is clearly demonstrated. (b) Polarization interference at $|\Phi^{(+)}\rangle$. A_2 is fixed at $\theta_2 = 45^\circ$ and A_3 is rotated, i.e. θ_3 is varied. High-visibility quantum interference (high degree of entanglement between photon 2 and photon 3) is clearly demonstrated.

4. Experimental set-up: Bell state measurement

The BSM consists of four SFG nonlinear crystals, two 45° projectors (G_1 and G_2), four single-photon counting detectors (D_4^I , D_4^{II} , D_4^{III} , and D_4^{IV}) and two compensators as well as other necessary optical components. The input photon (800 nm) and photon 2 (885 nm) may either interact in the two type-I or in the two type-II SFG crystals. Two pairs of lenses (L) are used as telescopes to focus the input beams onto the crystals. The vertical (horizontal) polarized amplitudes of the input photon (800 nm) and the vertical (horizontal) polarized photon 2 (885 nm) interact in the first (second) type-I SFG to generate a 420 nm horizontal (vertical) polarized photon. The horizontal (vertical) polarized amplitudes of the input photon and the vertical (horizontal) polarized photon 2 interact in the first (second) type-II SFG to generate a 420 nm horizontal (vertical) polarized photon. The 420 nm photons generated in the type-I SFG process is reflected to detectors D_4^I and D_4^{II} (after passing through C-2 and a 45° polarization projector G_1) by a dichroic beamsplitter DBS_2 and similarly for the 420 nm photons created in two type-II SFG processes. It is very important to design and adjust the Compensators (C-2 and C-3) correctly in order to make the horizontal and the vertical components of the 420 nm SFG quantum mechanically indistinguishable and to attain the expected relative phase.

Let us discuss the compensators C-2 and C-3 in detail. The time delay resulting from the Bell state measurement (sum frequency generation) process

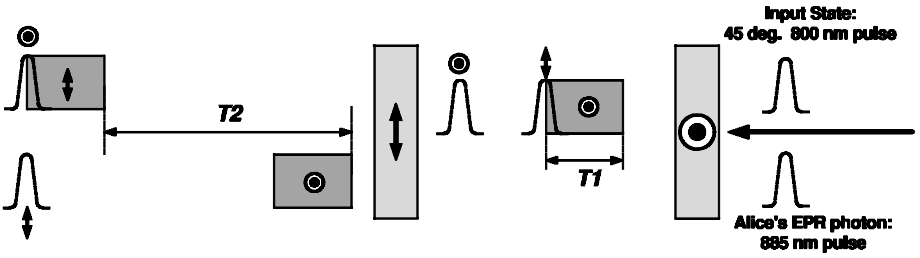


Figure 7. Time delay resulting from the Bell state measurement (sum frequency generation) process with two type-I BBO crystals. Input pulse is 45° linearly polarized 800 nm pulse. (One can assume arbitrary polarization also.) Alice's SPDC photon is 885 nm. The dispersion between the 800 nm and 885 nm photons is ignored for simplicity. SFG photons are distributed equally during the overlap of the two input pulses. Note that the SFG photons are delayed in time relative to the input pulses. The time distribution of the SFG photon is equal to T_1 . After two SFG crystals, the two SFG amplitudes are separated by T_2 . Compensator C-2 should overlap these two amplitudes.

using type-I BBO crystals is depicted in figure 7. The input pulse is a 45° polarized 800 nm femtosecond pulse. Alice's SPDC photon is 885 nm. We can ignore the dispersion between the two wavelengths and treat both of them as 800 nm. This is because both 885 nm and 800 nm photons should be polarized in the same way in the SFG process. Since they have the same polarization, the group velocities of 885 nm and 800 nm do not differ much. In type-II SFG process, this simplification does not work, however.

After the first crystal, the input pulse is split into two time-distinguishable pulses: one vertical and the other horizontal. If the crystal is thin, they may still overlap in time. However, for 2-mm-thick BBO crystals, they are separated more than the coherence time of the pulses themselves. Once they are separated in time more than the coherence times, there cannot be any more SFG process. Clearly, the horizontal polarized pulse is more advanced in time than the vertically polarized pulse. Since the SFG process occurs only when the two pulses overlap inside the crystal, the SFG photons (420 nm) acquire time distribution equal to T_1 and it is delayed with respect to the 800 nm photons. The SFG photons are horizontally polarized. In the second BBO crystal, the two 800 nm pulses start to overlap and generate SFG photons. After the second BBO crystal, the two 800 nm pulses completely overlap in time and the SFG photons are delayed with the time distribution equal to T_1 . The SFG photons are now vertically polarized. The separation in time between the two SFG photons is T_2 . T_1 and T_2 are easily calculated as,

$$T_1 = L \times \left[\frac{1}{u_o(800)} - \frac{1}{u_e(420)} \right],$$

$$T_2 = L \times \left[\frac{1}{u_o(420)} - \frac{1}{u_e(800)} \right],$$

where L is the crystal thickness. For a set of 2 mm type-I BBO crystals, $T_1 = 280$ fs and $T_2 = 763$ fs. C-2 should compensate T_2 exactly so that two SFG amplitudes overlap in time with a proper phase.

The SFG process in type-II crystals is a little more complicated. Suppose that a set of type-II BBO crystals is used for the Bell state measurement. In a type-II process, two input photons are orthogonally polarized. Therefore, in the first type-II BBO crystal,

$$885(e) + 800(o) \rightarrow 420(e).$$

Owing to the huge group velocity difference between e- and o-polarization in a type-II BBO, two input photons separate much more than the coherence time of the 800 nm input pulse. This means that no SFG can occur in the second crystal. For example, in a type-II BBO crystal,

$$\left[\frac{1}{u_e(885)} - \frac{1}{u_o(800)} \right] \times L = 265 \text{ fs} \quad (L = 1.5 \text{ mm}).$$

This value is much bigger than the coherence time of the 800 nm input pulse. However, it is smaller than the coherence time, ≈ 600 fs, of the 885 nm SPDC photons, see [22]. Therefore, it is possible to use type-II BBO crystals for the Bell state measurement, at least in principle.

There is, however, another problem with type-II BBO crystals. The walk-off angle is much bigger than that of type-I BBO crystals. Therefore, the SFG from the first crystal and the SFG from the second crystal will be spatially separated. Such a spatial mode separation should be prevented or minimized to insure high-fidelity teleportation. On average, type-II SFG in a BBO crystal experiences walk-off angle of 75 mrad and the effective $d_{\text{eff}} \approx 1.3 \text{ pm V}^{-1}$. On the other hand, type-II LBO crystals have much smaller walk-off angle. On average, the walk-off angle is $6 \sim 9$ mrad and d_{eff} is approximately three to six times lower for the wavelengths of interest. We choose, therefore, to work with type-II LBO crystals in the second part of the Bell state measurement process. The time separation between two input pulses in a type-II SFG process in a LBO crystal is (note that LBO is a biaxial crystal)

$$885(e) + 800(o) \rightarrow 420(o),$$

$$T_3 \equiv \left[\frac{1}{u_e(885)} - \frac{1}{u_o(800)} \right] \times L = 200 \text{ fs} \quad (L = 1.5 \text{ mm}), \quad (17)$$

which is smaller than the time separation resulting from a type-II BBO crystal.

Figure 8 shows the time distribution of the amplitudes involved in the SFG process with two type-II LBO crystals. The 800 nm input pulse has a pulse width of 100 fs and the 885 nm SPDC photons have an effective pulse width of 600 fs. Suppose that the 800 nm and 885 nm pulse enters the first crystal in the way shown in figure 8. The vertical and horizontal components of the 885 nm pulse and 800 nm pulse are separated in time after the first crystal. The time distribution of the SFG photons is given by

$$T_4 \equiv \left[\frac{1}{u_o(800)} - \frac{1}{u_e(420)} \right] \times L. \quad (18)$$

After the second type-II LBO crystal, the horizontal and vertical components of 800 nm and 885 nm pulses now overlap in time. However, the SFG amplitudes from the first and second crystals are separated in time by

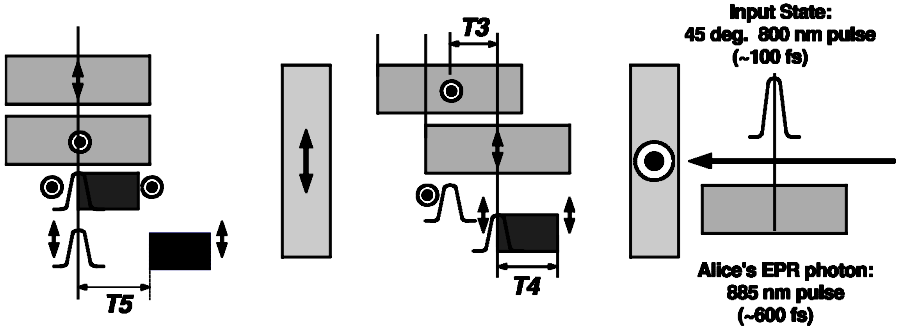


Figure 8. Time delay resulting from the Bell state measurement (sum frequency generation) process with two type-II LBO crystals. Input pulse is an arbitrarily polarized 800 nm pulse (pulse width ≈ 100 fs). Alice's SPDC photon is 885 nm (time distribution ≈ 600 fs). The dispersion between 800 nm and 885 nm photons cannot be ignored in type-II processes. SFG photons are distributed equally during the overlap of the two input pulses. The time distribution of the SFG photon is equal to T_4 . After two SFG crystals, the two SFG amplitudes are separated by T_5 . Compensator C-3 should overlap these two amplitudes.

$$T_5 \equiv \left[\frac{1}{u_e(420)} - \frac{1}{u_e(800)} \right] \times L. \quad (19)$$

In the experiment we used a 1.5-mm-thick type-II LBO crystal. Therefore, $T_4 = 240$ fs and $T_5 = 271$ fs. Compensator C-3 should compensate T_5 so that the two SFG wavepackets overlap in time.

5. Experimental set-up: sum frequency generation

Since the input state (photon 1) and photon 2 should overlap inside the SFG crystals exactly, a prism is used to adjust the path-length of the input pulse, see figure 5. The 800 nm input pulse and 400 nm pump pulse (which pumps the SPDC crystals) are actually drawn from a single Ti:Sapphire laser to ensure that they have the same repetition rate (82 MHz). M_1 is a dichroic mirror which reflects the 800 nm photons while transmitting the 885 nm ones. To be sure that the SFG process occurs with a single photon input, we measured the coincidence counting rate between one of Alice's detectors and Bob's detector D_3 by moving the position of the prism. Figure 9 shows a typical data curve of the measurement. It is clear that SFG occurs only when the input pulse (photon 1) and photon 2 (single photon created by the SPDC process) overlap perfectly inside the SFG crystals.

6. Discussions

It should be noted that the efficiency in the teleportation measurement is a lot lower than the SFG demonstration. The reason why we get such a low coincidence counting rate in figures 3 and 4 compared with figure 9 is that very small pinholes have to be placed in front of Alice's detectors for the teleportation measurement to

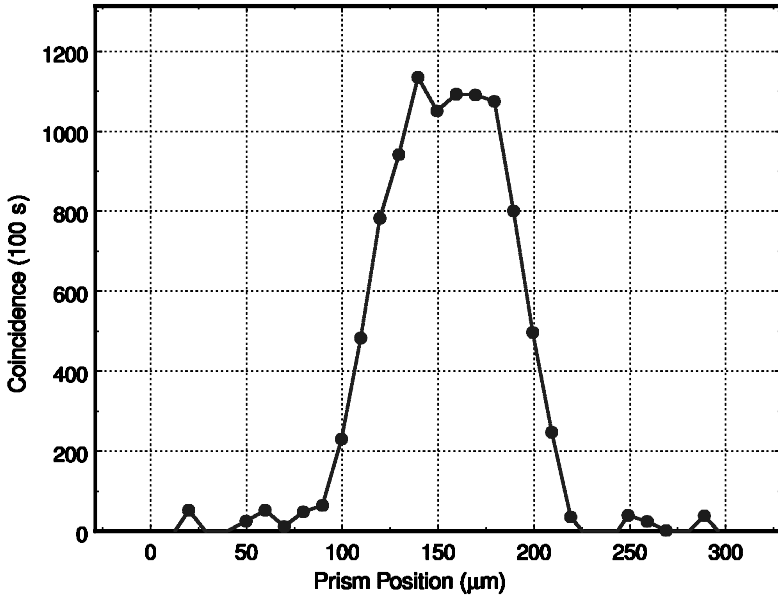


Figure 9. SFG measurement as a function of the prism position. SFG is observed only when the input pulse and the SPDC photons overlap exactly inside the crystals. The efficiency of SFG (from the SPDC photons) is roughly estimated to be 0.1~1%. The SFG crystals used for the data shown in this paper are BBOs with 2-mm thickness.

ensure good spatial mode overlap. We are currently in the process of improving the collection efficiencies.

Let us now discuss the fidelity of teleportation. The teleportation fidelity F is defined to be the overlap between the incoming ($|\psi_i\rangle$) and outgoing ($|\rho_f\rangle$) states: $F = \langle \psi_i | \rho_f | \psi_i \rangle$. Since the input state is a pure state, the calculation of F is greatly simplified. From the measurements, it is concluded that the output states have the expected polarization with some unpolarized components. The teleportation fidelity can be calculated from the visibility of the data. The experimentally achieved fidelity $F \approx 0.83$.

In this experiment, femtosecond laser pulses have been used to prepare the input state to reduce data collection time. Recent research on nonlinear optics at low light levels may enable high-efficiency SFG at the single-photon level in the future [25].

References

- [1] WOOTERS, W. K., and ZUREK, W. H., 1982, *Nature*, **299**, 802.
- [2] BENNETT, C. H., BRASSARD, G., CRÉEAU, C., JOZSA, R., PERES, A., and WOOTERS, W. K., 1993, *Phys. Rev. Lett.*, **70**, 1895.
- [3] EINSTEIN, A., PODOLSKY, B., and ROSEN, N., 1935, *Phys. Rev.*, **47**, 777.
- [4] BOUWMEESTER, D., PAN, J.-W., MATTLE, K., EIBL, M., WEINFURTER, H., and ZEILINGER, A., 1997, *Nature*, **390**, 575.
- [5] BOSCHI, D., BRANCA, S., DE MARTINI, F., HARDY, L., and POPESCU, S., 1998, *Phys. Rev. Lett.*, **80**, 1121.

- [6] FURUSAWA, A., SØRENSEN, J. L., BRAUNSTEIN, S. L., FUCHS, C. A., KIMBLE, H. J., and POLZIK, E. S., 1998, *Science*, **282**, 706.
- [7] KIM, Y.-H., KULIK, S. P., and SHIH, Y. H., 2001, *Phys. Rev. Lett.*, **86**, 1370.
- [8] KLYSHKO, D. N., 1998, *Phys. Usp.*, **41**, 885.
- [9] KLYSHKO, D. N., 1998, *JETP*, **87**, 639.
- [10] KLYSHKO, D. N., 1998, *Phys. Lett. A*, **247**, 261.
- [11] VAIDMAN, L., and YORAN, N., 1999, *Phys. Rev. A*, **59**, 116.
- [12] LÜTKENHAUS, N., CALSAMIGLIA, J., and SUOMINEN, K.-A., 1999, *Phys. Rev. A*, **59**, 3295.
- [13] KWIAT, P. G., and WEINFURTER, H., 1998, *Phys. Rev. A*, **58**, R2623.
- [14] SCULLY, M. O., ENGLERT, B.-G., and BEDNAR, C. J., 1999, *Phys. Rev. Lett.*, **83**, 4433.
- [15] VITALI, D., FORTUNATO, M., and TOMBESI, P., 2000, *Phys. Rev. Lett.*, **85**, 445.
- [16] PARIS, M. G. A., PLENIO, M. B., BOSE, S., JONATHAN, D., and D'ARIANO, G. M., 2000, *Phys. Lett. A*, **273**, 153.
- [17] DELRE, E., CROSIGNANI, B., and DI PORTO, P., 2000, *Phys. Rev. Lett.*, **84**, 2989.
- [18] BENNETT, C. H., and WIESNER, S. J., 1992, *Phys. Rev. Lett.*, **69**, 2881.
- [19] MATTLE, K., WEINFURTER, H., KWIAT, P. G., and ZEILINGER, A., 1996, *Phys. Rev. Lett.*, **76**, 4656.
- [20] ZUKOWSKI, M., ZEILINGER, A., HORNE, M. A., and EKERT, A. K., 1993, *Phys. Rev. Lett.*, **71**, 4287.
- [21] PAN, J.-W., BOUWMEESTER, D., WEINFURTER, H., and ZEILINGER, A., 1998, *Phys. Rev. Lett.*, **80**, 3891.
- [22] KIM, Y.-H., KULIK, S. P., and SHIH, Y. H., 2000, *Phys. Rev. A*, **61**, 011802(R).
- [23] KIM, Y.-H., KULIK, S. P., and SHIH, Y. H., 2001, *Phys. Rev. A*, **63**, 060301 (R).
- [24] KIM, Y.-H., CHEKHOVA, M. V., KULIK, S. P., RUBIN, M. H., and SHIH, Y. H., 2001, *Phys. Rev. A*, **63**, 062301.
- [25] HARRIS, S. E., and HAU, L. V., 1999, *Phys. Rev. Lett.*, **82**, 4611.